EPJ Web of Conferences **141**, 02004 (2017) DOI: 10.1051/epjconf/201714102004
ISMD 2016

Low energy exclusive $e^+e^- \rightarrow$ hadrons cross sections and g − 2 of the muon

J. William Gary[1,a]

[1] *Department of Physics and Astronomy, University of California, Riverside, CA 92521, USA*

Abstract. The 3.5 standard deviation discrepancy between the standard model prediction for the muon anomalous magnetic moment $g-2$ and the corresponding experimental measurement is one of the most intriguing potential signals for physics beyond the standard model. The largest uncertainty in the standard model prediction for the muon $g-2$ arises from uncertainties in the measured low-energy $e^+e^- \rightarrow$ hadrons cross sections. New cross section results from the Babar experiment at SLAC for $e^+e^- \rightarrow \pi^+\pi^-\pi^0\pi^0$ and for $e^+e^- \rightarrow KK\pi\pi$ channels are presented that significantly reduce some of the uncertainties in the standard model prediction for the muon $g-2$.

1 Introduction

The gyromagnetic ratio g specifies the relationship between an angular momentum and the corresponding magnetic moment. The Dirac result for the gyromagnetic ratio g_ℓ of an elementary charged spin-1/2 lepton ℓ is $g_\ell = 2$ exactly. The Dirac result corresponds to the tree level diagram shown in the leftmost plot of Fig. 1. Radiative corrections alter the prediction to $g_\ell = 2(1 + a_\ell)$, introducing sensitivity to new physics through loops. The term a_ℓ is known as the anomalous moment, expressed as $a_\ell = (g_\ell - 2)/2$ and simplified in common parlance to "$g - 2$". The muon anomaly a_μ is much more sensitive to virtual heavy particle production in loops than the electron anomaly a_e because the relative virtual terms scale like $(m_\mu/m_e)^2 \approx 43,000$, with m_ℓ the lepton mass.

In the standard model (SM), the muon anomaly can be expressed as $a_\mu = a_\mu^{QED} + a_\mu^{EW} + a_\mu^{had}$, receiving contributions from electromagnetic, weak, and hadronic loop corrections. The purely electromagnetic term a_μ^{QED} has been calculated [2] to high order in perturbation theory. The electroweak term a_μ^{EW} [3] includes contributions from the recently discovered Higgs boson. The hadronic term a_μ^{had} is itself divided into three parts, illustrated by the three rightmost plots of Fig. 1: the leading-order hadronic vacuum polarization term $a_\mu^{had,LO-VP}$, the higher-order hadronic vacuum polarization terms $a_\mu^{had,HO-VP}$, and the so-called light-by-light scattering term $a_\mu^{had,LbLs}$. A summary of the individual contributions to the SM result for a_μ is given in Table 1. Summing these contributions yields a total SM prediction of $a_\mu^{SM} = 1\,16\,591\,802 \pm 49 \times 10^{-11}$ [4], which lies $287 \pm 80 \times 10^{-11}$ below the average measured result, $a_\mu^{data} = 1\,16\,592\,091 \pm 63 \times 10^{-11}$ [5, 6], corresponding to a discrepancy of about 3.5 standard deviations. From Table 1 it is seen that the uncertainty in the SM prediction is dominated by the uncertainty in the leading-order vacuum polarization term $a_\mu^{had,LO-VP}$.

[a] e-mail: bill.gary@ucr.edu

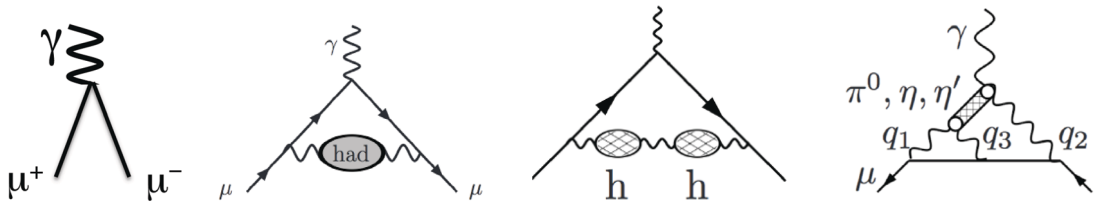

Figure 1. (left) Tree-level vertex diagram for a muon coupling to a photon and (left-center) the diagram corresponding to the leading-order hadronic correction. Examples of diagrams for the higher-order hadronic corrections and for light-by-light scattering are shown in the right-center and right plots, respectively. The three leftmost plots are taken from Ref. [1].

Table 1. SM results for the different contributions to the muon anomaly a_μ, taken from Ref. [4].

a_μ term	SM prediction ($\times 10^{-11}$)
a_μ^{QED}	116584718.951 ± 0.080
a_μ^{EW}	153.6 ± 1.0
$a_\mu^{had,LO-VP}$	6923 ± 42
$a_\mu^{had,HO-VP}$	−98.4 ± 0.7
$a_\mu^{had,LbLs}$	105 ± 26

The energy scale is too low for $a_\mu^{had,LO-VP}$ to be calculated perturbatively, and lattice calculations [7] are not yet sufficiently precise. Instead, the most precise result for $a_\mu^{had,LO-VP}$ is currently obtained from low-energy $e^+e^- \to hadrons$ data, using the optical theorem and the following dispersion integral (see Ref. [6]):

$$a_\mu^{had,LO-VP} = \left(\frac{\alpha}{3\pi}\right)^2 \int_{m_\pi^2}^{\infty} \frac{K(s)R_{had}}{s} ds, \tag{1}$$

where $K(s)$ is a kinematic factor and R_{had} is the $e^+e^- \to hadrons$ cross section normalized to the Born-level $e^+e^- \to \mu^+\mu^-$ cross section. Because of the $1/s$ factor, low-energy contributions dominate the dispersion integral. Therefore precise measurements of R_{had} are needed at low values of center-of-mass energy $\sqrt{s}$. Below $\sqrt{s} = 2$ GeV, the sum of exclusive hadronic channels is used because the background from $e^+e^- \to e^+e^-$ and $e^+e^- \to \mu^+\mu^-$ events is difficult to distinguish from inclusive multihadronic events at such low energies. Also, the inclusive detection efficiency is difficult to determine with precision at very low $\sqrt{s}$. For energies above 2 GeV, inclusive $e^+e^- \to hadrons$ data and perturbative calculations can be used.

Figure 2 shows measurements of exclusive hadronic cross sections from the Babar Collaboration at SLAC. It is seen that the $e^+e^- \to \pi^+\pi^-$ channel dominates the low-energy hadronic cross section. It contributes about 75% of the area to the dispersion integral. The $e^+e^- \to \pi^+\pi^-$ cross section has been measured by the Babar [8], KLOE [9, 10], and BES-III [11] experiments, each claiming around 1% precision in their results. However, the results of the three experiments differ in some kinematic regions by more than the claimed 1% uncertainties. Future results, expected from the Babar, BES-III, and CMD3 experiments, may clarify the $e^+e^- \to \pi^+\pi^-$ results.

Table 2 lists the channels whose uncertainties in the cross section contribute the most to the uncertainty $\Delta a_\mu^{had,LO-VP}$ in $a_\mu^{had,LO-VP}$. The largest contribution to $\Delta a_\mu^{had,LO-VP}$ comes from the $\pi^+\pi^-$ channel, followed by the $\pi^+\pi^-\pi^0$ and $\pi^+\pi^-\pi^0\pi^0$ channels. Channels with two kaons are also seen

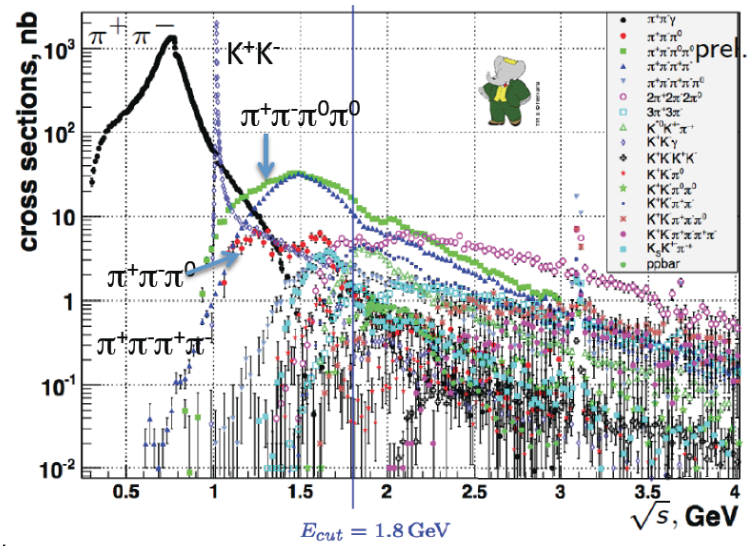

Figure 2. Summary of Babar measurements of low-energy exclusive hadronic cross sections.

to be important. Babar has recently measured the cross sections for $e^+e^- \to K^+K^-$ [12, 13] and $e^+e^- \to K_L K_S$ [14]. These new results will significantly reduce the respective contributions to $\Delta a_\mu^{had,LO-VP}$.

In the following, new Babar measurements of the $e^+e^- \to \pi^+\pi^-\pi^0\pi^0$, $K_S K^+\pi^-\pi^0$, $K_S K^+\pi^-\eta$, $K_S K_L\pi^0$, $K_S K_L\eta$, and $K_S K_L\pi^0\pi^0$ cross sections are presented, and the implications for $\Delta a_\mu^{had,LO-VP}$ discussed. These results are preliminary. The data are collected with the initial-state radiation (ISR) method. In the ISR method, an effective reduced hadronic energy $\sqrt{s'}$ is obtained by selecting events with a hard ISR photon radiated from either the incoming electron or incoming positron in fixed-energy e^+e^- collisions. In the Babar studies, the ISR photon candidate is taken to be the highest energy photon in an event and must have a center-of-mass energy larger than 3 GeV.

Table 2. Exclusive $e^+e^- \to$ *hadrons* channels contributing the largest uncertainty $\Delta a_\mu^{had,LO-VP}$ to the SM prediction of the muon anomaly term $a_\mu^{had,LO-VP}$ (taken from Ref. [4]).

Channel	$\pi^+\pi^-$	$\pi^+\pi^-\pi^0$	$\pi^+\pi^-\pi^0\pi^0$	K^+K^-	$\pi^+\pi^-\pi^+\pi^-$	$KK\pi\pi$	$K_S K_L$
$\Delta a_\mu^{had,LO-VP}$ ($\times 10^{-11}$)	28	15	12	7	5	4	4

2 The $e^+e^- \to \pi^+\pi^-\pi^0\pi^0$ cross section

As illustrated in Table 2, the $e^+e^- \to \pi^+\pi^-\pi^0\pi^0$ process represents one of the least known cross sections important for the muon anomaly. In the Babar analysis, events with exactly two oppositely charged tracks are selected. The two tracks must have momentum $p > 100$ MeV and be consistent with originating at the primary event vertex. Besides the ISR photon candidate, there must be at least four other photon candidates in the event, each with energy $E > 50$ MeV. A kinematic fit is performed to the signal hypothesis, constraining two 2γ combinations to the π^0 mass. The overall combination of four photons that yields the smallest χ^2 value is selected, requiring $\chi^2 < 30$.

Background from the ISR processes $e^+e^- \to \pi^+\pi^-\pi^0\gamma$, $e^+e^- \to \pi^+\pi^-\pi^0\eta\gamma$, and $e^+e^- \to \pi^+\pi^-\eta\eta\gamma$ is suppressed by rejecting events with kinematic fits consistent with those hypotheses. Background from ISR $e^+e^- \to \pi^+\pi^-\pi^0\pi^0\pi^0\gamma$ events is evaluated by measuring the cross section for these events using an analogous technique to that described above for $e^+e^- \to \pi^+\pi^-\pi^0\pi^0\gamma$ events, and then adjusting the simulation accordingly to reliably predict the rate of these events in the $e^+e^- \to \pi^+\pi^-\pi^0\pi^0\gamma$ sample. The largest non-ISR background is from $q\bar{q}$ continuum events arising from the misidentification of a photon from π^0 decay as an ISR photon. This background is subtracted using simulation that is normalized to data based on the π^0 peak from $\gamma_{ISR}\gamma$ combinations, where γ_{ISR} is the ISR photon candidate, with γ any other photon in the event not assigned to a signal π^0 candidate.

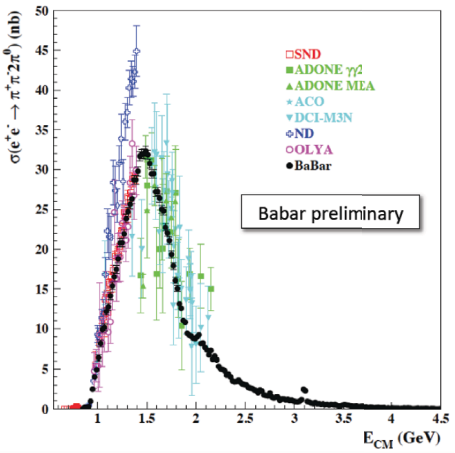

Figure 3. Babar measurement of the $e^+e^- \to \pi^+\pi^-\pi^0\pi^0$ cross section in comparison with published results from previous experiments.

The resulting measurement of the $e^+e^- \to \pi^+\pi^-\pi^0\pi^0$ cross section is shown in Fig. 3. The Babar results are far more precise than previously published results, and cover a wider energy range. The contribution to the muon anomaly for $1.02 < \sqrt{s} < 1.8$ GeV is measured with 3.4% precision, compared to the previous precision of 6.7% based on preliminary Babar data from 2007.

3 First measurements of the $e^+e^- \to K_S K^+\pi^-\pi^0$ and $K_S K^+\pi^-\eta$ cross sections

A similar analysis is performed for the $e^+e^- \to K_S K^+\pi^-\pi^0$ and $K_S K^+\pi^-\eta$ cross sections. Besides the ISR photon candidate, at least one $K_S \to \pi^+\pi^-$ candidate consistent with the interaction point, and at least two additional photons with a diphoton mass consistent with the π^0 or η mass, are required. Two oppositely charged tracks must be present, one identified as a pion and the other as a kaon. Background from non-ISR $q\bar{q}$ events is evaluated from simulation normalized to data using the $\gamma_{ISR}\gamma$ peak at the π^0 mass. Background from ISR processes is evaluated from data sidebands.

The resulting cross section measurements are shown in Fig. 4. These are the first measurements of these cross sections. Very clear J/ψ peaks are visible for both channels The $J/\psi \to K_S K^+\pi^-\pi^0$ branching fraction is measured to be $(5.7 \pm 0.3 \pm 0.4) \times 10^{-3}$, where the first uncertainty is statistical and the second systematic. This is the first observation of this decay channel. The $J/\psi \to K_S K^+\pi^-\eta$

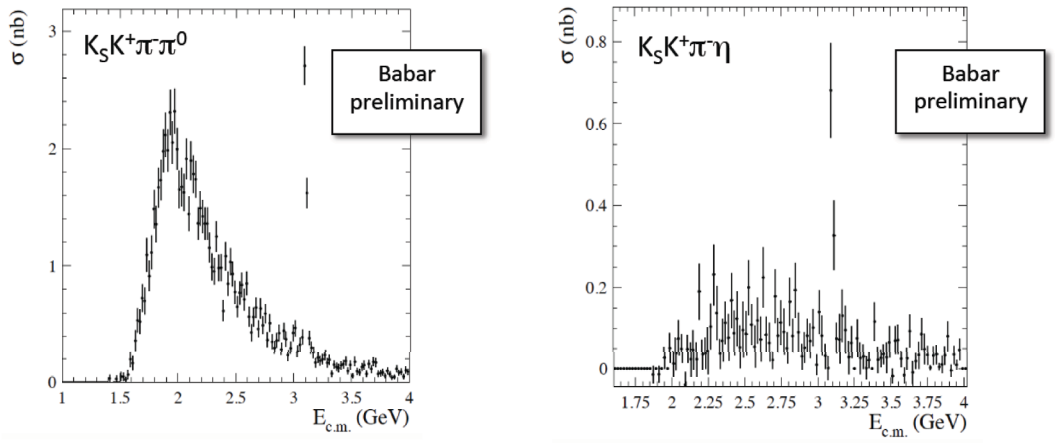

Figure 4. Babar measurements of the (left) $e^+e^- \to K_S K^+\pi^-\pi^0$ and (right) $K_S K^+\pi^-\eta$ cross sections.

branching fraction is measured to be $(1.30 \pm 0.25 \pm 0.07) \times 10^{-3}$, around 2 standard deviations below a previous result from the BES Collaboration [15].

4 First measurements of the $e^+e^- \to K_S K_L\pi^0$, $K_S K_L\eta$, and $K_S K_L\pi^0\pi^0$ cross sections

As in the analysis described in the previous section, at least one $K_S \to \pi^+\pi^-$ candidate and at least two additional photons consistent with π^0 or η decay are required. A K_L candidate is identified as an isolated calorimeter cluster with energy larger than 0.2 GeV. The detection efficiency for K_L particles is determined from data using $e^+e^- \to \phi\gamma \to K_S K_L\gamma$ events and a tag-and-probe method. Background is suppressed, with the residual background subtracted, using methods similar to those described in the previous sections.

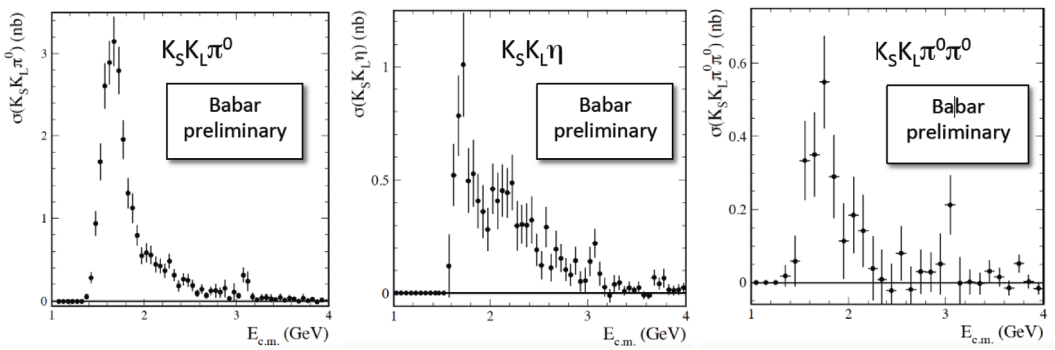

Figure 5. Babar measurements of the (left) $e^+e^- \to K_S K_L\pi^0$, (center) $K_S K_L\eta$, and (right) $K_S K_L\pi^0\pi^0$ cross sections.

The cross section results are shown in Fig. 5. All of these are first measurements. The corresponding J/ψ branching fractions, $(2.06 \pm 0.24 \pm 0.10) \times 10^{-3}$, $(1.45 \pm 0.32 \pm 0.08) \times 10^{-3}$, and $(1.86 \pm 0.43 \pm 0.10) \times 10^{-3}$, respectively, also represent first measurements.

5 Implications of $\mathbf{KK\pi\pi}$ measurements on $\mathbf{a}_\mu$

The results for $e^+e^- \to K_S K^+\pi^-\pi^0$ and $K_S K_L\pi^0\pi^0$ presented above can be combined with previous Babar results for $e^+e^- \to K^+K^-\pi^+\pi^-$, $K^+K^-\pi^0\pi^0$, $K_S K_S\pi^+\pi^-$, and $K_S K_L\pi^+\pi^-$ [14, 16], which all include studies of the intermediate resonant states, to calculate the contribution of $KK\pi\pi$ channels to the muon anomaly a_μ. Heretofore, the contributions of these previously unmeasured channels had been estimated using isospin relations. The contribution of $KK\pi\pi$ channels to a_μ for $\sqrt{s} < 1.8$ GeV is determined to 6% precision, compared to 30% precision available previously.

6 Summary

Precise low-energy e^+e^- hadronic cross section data are needed to obtain an accurate standard model prediction for the part of the muon magnetic moment anomaly associated with leading-order vacuum polarization terms. New results from the Babar experiment at SLAC reduce the respective uncertainty in this term from 6.7% to 3.4% for the $\pi^+\pi^-\pi^0\pi^0$ channel and from 30% to 6% for $KK\pi\pi$ channels. Besides the implications for the muon anomaly, the Babar ISR program has provided new tests of QCD, such as in measurements of koan form factors, a wealth of information about low-mass resonances, first observations of cross sections, and first observations of J/ψ and $\psi(2S)$ branching fractions.

References

[1] F. Jegerlehner and A. Nyffeler, Phys. Rept. **477**, 1 (2009).
[2] T. Aoyama, M. Hayakawa, T, Kinoshita, and M. Nio, Phys. Rev. Lett. **109**, 111808 (2012).
[3] C. Gnendiger, D. Stöckinger, and H. Stöckinger-Kim, Phys. Rev. D **88**, 053005 (2013).
[4] M. Davier, A. Hoecker, B, Malaescu, and Z. Zhang, Z. Phys. C **71**, 1515 (2011).
[5] G. W. Bennett et al. (E821 Collaboration), Phys. Rev. D **73**, 072003 (2006).
[6] K. A. Olive et al. (Particle Data Group), Chin. Phys. C **38**, 090001 (2014).
[7] M. Della Morte, B. Jäger, A. Jüttner, and H. Wittig, JHEP **03**, 055 (2012).
[8] J. P. Lees et al. (Babar Collaboration), Phys. Rev. D **86**, 032013 (2012).
[9] F. Ambrosino et al. (KLOE Collaboration), Phys. Lett. B **700**, 102 (2011).
[10] D. Babusci et al. (KLOE Collaboration), Phys. Lett. B **720**, 336 (2013).
[11] M. Ablikim et al. (BESIII Collaboration), Phys. Lett. B **753**, 629 (2016).
[12] J. P. Lees et al. (Babar Collaboration), Phys. Rev. D **88**, 032013 (2013).
[13] J. P. Lees et al. (Babar Collaboration), Phys. Rev. D **92**, 072008 (2015).
[14] J. P. Lees et al. (Babar Collaboration), Phys. Rev. D **89**, 092002 (2014).
[15] M. Ablikim et al. (BES Collaboration), Phys. Rev. D **77**, 032005 (2008).
[16] J. P. Lees et al. (Babar Collaboration), Phys. Rev. D **86**, 012008 (2012).